Advances in Military Technology
Vol. 20, No. 2, 2025, pp. 585-599
ISSN 1802-2308, eISSN 2533-4123
DOI 10.3849/aimt.02004

Comparative Analysis of Next-Gen Single-Crystal Nickel Superalloys for HPT Blades via FEM

A. S. Sait[1], and S. A. Rabbani[2*]

[1] *Department of Mechanical Engineering Technology, Yanbu Industrial College, Yanbu Alsinayiah 46451, Saudi Arabia*
[2] *School of Mechanical and Electrical Engineering, University of Electronics Science and Technology of China (UESTC), Chengdu, China*

The manuscript was received on 16 June 2025 and was accepted after revision for publication as an original research paper on 13 December 2025.

Abstract:

This study details a structural integrity evaluation of a high-pressure turbine (HPT) blade made up of three nickel-based single-crystal superalloys, specifically CMSX-4, CMSX-8, and CMSX-4 Plus. Finite element analysis was conducted to evaluate stress, strain, deformation, and safety factor under real thermal and mechanical loading. Aerodynamic precision was simulated in blade geometry, discretized using tetrahedral elements, and fixed root and surface pressure was applied. Material information was used from experimental sources. Results showed similar levels of stress for all alloys, but differences in strain and deformation were noted. CMSX-8 registered the lowest deformation and highest safety factor, indicating better mechanical performance and appropriateness as the material of choice for future high-performance turbine blades.

Keywords:

lightweight alloys, HPT blade, FEA, nickel-based superalloys, strain and deformation analysis

1 Introduction

High-pressure turbine (HPT) blades are critical components of sophisticated jet engines, which are exposed to severe conditions of high temperature, extensive mechanical stresses, and corrosive environments. Such conditions necessitate materials with the ability to maintain structural integrity, creep deformation resistance, and oxidation resistance during extended service life. The compulsion for enhanced engine

[*] *Corresponding author: School of Mechanical and Electrical Engineering, University of Electronic Science and Technology of China (UESTC), No. 2006 Xiyuan Avenue, High-Tech Zone, Chengdu, Sichuan, CN-611731, P. R. China. Phone: +86 1 9828 10 85 89, E-mail: sagharalirabbani@gmail.com. ORCID: 0009-0008-9606-7600.*

efficiencies and reduced emissions has also accelerated the development and research on advanced materials to withstand such extreme operating conditions.

Nickel-based single-crystal superalloys are emerging as the material of choice for HPT blades due to their enhanced high-temperature strength, creep, and corrosion resistance. Of these, CMSX-4, CMSX-8, and CMSX-4 Plus have been exhaustively tested and utilized. CMSX-4, a second-generation superalloy, has an optimal combination of the mechanical properties and ease of manufacture. CMSX-8 is a third-generation alloy in which rhenium is added for increased creep resistance. CMSX-4 Plus is a product derived from CMSX-4 for providing improved phase stability and performance at elevated temperatures [1].

Various aspects of these superalloys have been investigated by recent research studies. Investigations, for instance, have looked into how the micro-structure and mechanical properties of CMSX-4 are affected by laser shock peening, which showed surface hardness and crack initiation resistance enhancement [2]. Other studies have also investigated the stress corrosion behavior of CMSX-4 and its behavior in corrosive environments [3]. CMSX-4 turbine blade life prediction models have been developed, with thermo-mechanical loads and fatigue-creep interactions in mind, which are crucial for enhancing blade durability [4]. In addition, new approaches to repair, such as high-velocity air fuel (HVAF) spraying, have been explored for the recovery of the integrity of CMSX-4 components after service damage [5].

2 Literature Review

2.1 Development and Composition of CMSX Superalloys

The growing demand for more efficiency and performance in jet engines has provoked the creation of nickel-based single-crystal superalloys, and most notably the CMSX series. Developed as a second-generation alloy, CMSX-4 contains approximately 3 % rhenium and offers a combination of creep resistance and formability [1]. CMSX-8 is the third-generation alloy with higher rhenium content and balanced alloying additions such as tungsten and tantalum to develop greater high-temperature strength and phase stability [6]. Meanwhile, CMSX-4 Plus aimed to modify the initial CMSX-4 by reducing the γ/γ' lattice mismatch and increasing phase stability for exposures greater than 1 100 °C [7].

Alloying schemes, particularly control of the γ' phase fraction and elimination of undesirable phases such as TCP phases, have been instrumental to success with these alloys [8]. Modern computational thermodynamics techniques such as CALPHAD have made possible more effective prediction of phase stability and trace alloying element optimization to optimize CMSX-4 Plus for next-generation turbine applications.

2.2 Microstructural Characteristics and Evolution during Service

The improved mechanical performance of CMSX-4, CMSX-8, and CMSX-4 Plus is largely due to their microstructure with controlled ordered γ' (Ni_3Al) phase with a uniform distribution in the γ matrix. The γ' phase is the strengthening agent, providing resistance to dislocation motion at high temperatures [9].

Experiments on CMSX-4 have revealed that heat treatment conditions play a decisive role in determining precipitate size, distribution, and morphology of the γ'

precipitates, thus having direct implications on mechanical properties [10]. Elevated temperature thermal aging or long-term service exposure causes coarsening of the γ' phase and, under certain conditions, the nucleation of undesirable TCP phases, particularly in the more rhenium-contained alloys such as CMSX-8 [8].

Sophisticated characterization methods, including high-resolution transmission electron microscopy (HR-TEM) and atom probe tomography (APT), have identified nanoscale segregation behavior in CMSX-4 and CMSX-8 that is essential for phase stability upon high-temperature exposure. In CMSX-4 Plus, the decreased lattice misfit between the γ and γ' phases inhibit the nucleation of TCP phases, thereby prolonging the material's high-temperature service life [11].

In addition, research in creep deformation has indicated rafting of the γ' phase takes place due to long-time exposure to temperature and stress and leads to directionally coarsened structures which either improve or impair mechanical properties based on crystal orientation and state of stress.

2.3 Mechanical Properties of CMSX-4, CMSX-8, and CMSX-4 Plus

High-pressure turbine blade mechanical performance is particularly sensitive to tensile strength, creep resistance, fatigue life, and fracture toughness of the material. CMSX-4 was initially developed to be reliable up to ~1 100 °C with superior creep strength due to its high-volume fraction of γ' (~70 %) [12]. The development of CMSX-8, with increased rhenium and tantalum levels, provided additional creep rupture life and low-cycle fatigue strength improvement at high temperatures.

Recent research has characterized the room temperature and high-temperature tensile properties of CMSX-4 and CMSX-8 and found that CMSX-8 shows greater tensile yield stress and ultimate tensile strength at temperatures above 900 °C than CMSX-4 [13]. CMSX-4 Plus demonstrates improved mechanical stability under cyclic loading conditions because of fine microstructure and improved defect nucleation suppression during service.

Regarding fatigue behavior, the development of fatigue cracks at the γ/γ' interfaces continues to be a major concern. Nevertheless, CMSX-8 exhibits retardation in crack initiation and reduced rates of propagation, particularly under thermomechanical fatigue testing conditions that reflect jet engine operational environments [14]. Concurrently, innovations in alloying concepts for CMSX-4 Plus have enabled improved mechanical property retention following extensive cyclic exposure.

The anisotropic behavior of single-crystal superalloys also significantly contributes to mechanical performance. Recent research emphasizes that [001]-oriented CMSX-4 and CMSX-8 samples yield maximum creep and tensile performance based on alignment with the main slip systems of nickel.

2.4 Thermal Properties and High-Temperature Performance

Thermal characteristics like thermal conductivity, thermal expansion coefficient, and oxidation resistance are essential for the stable operation of HPT blades. CMSX-4 has been reported to exhibit constant thermal conductivity over a broad temperature range, though minor decreases are noted above 1 000 °C due to microstructural coarsening [15].

CMSX-8, on the other hand, has slightly reduced thermal conductivity but considerably improved oxidation resistance due to the optimization of chromium and aluminum contents that supports the development of protective oxide scales [16]. Research has proven that the introduction of elements such as rhenium (Re) and

ruthenium (Ru) in CMSX-8 slows diffusion processes, slowing down the rates of oxidation and thermal degradation over extended service.

CMSX-4 Plus improves on these areas even further by raising the γ' solvus temperature, thus widening the operating temperature range above 1 150 °C without early microstructural degradation [17]. Current research shows that CMSX-4 Plus exhibits better cyclic oxidation resistance than both CMSX-4 and CMSX-8, especially under thermomechanical fatigue conditions common in jet engines.

Another significant thermal property of turbine blade materials is the coefficient of thermal expansion (CTE). Incompatibility of CTE between the blade material and thermal barrier coatings (TBCs) can result in premature coating delamination. Both CMSX-4 and CMSX-8 exhibit comparatively compatible CTEs with typical TBC systems such as yttria-stabilized zirconia (YSZ) [18], though CMSX-4 Plus has slightly better compatibility, which may increase the life of coated blades.

2.5 Creep and Fatigue Resistance

Creep and fatigue are prevalent failure modes for high-pressure turbine (HPT) blades subjected to high temperatures and cyclic loading. Hence, the evolution of alloys like CMSX-4, CMSX-8, and CMSX-4 Plus has greatly emphasized increasing resistance to these damage mechanisms.

CMSX-4 has been well-known for its superior creep resistance at temperatures of up to 1 100 °C. This is due to a combination of high-volume fraction of γ' and optimized solid-solution strengthening by refractory elements such as rhenium (Re) and tungsten (W) [19]. Its creep rupture strength, however, drops considerably when exposed to long-term exposures at temperatures higher than its design limit, which has driven the creation of better variants.

CMSX-8 was developed with higher rhenium content than CMSX-4, and it further raises its creep strength by retarding dislocation mobility and diffusion behavior. High-resolution examinations have determined that CMSX-8 possesses longer creep life at stresses comparable to those encountered in contemporary aero-engine operation [20].

CMSX-4 Plus builds on these developments by adding platinum group metals (PGMs) and minor adjustments to the balance of the alloy. This results in stabilization of the γ/γ' microstructure on prolonged creep exposure as well as retarding rafting effects that would otherwise reduce the material's strength. Its creep rupture life has been documented at over 1 000 hours at 1 100 °C and 137 MPa, higher than both CMSX-4 and CMSX-8 under the same conditions [19].

3 Methodology

The strategy for structural integrity analysis of CMSX-4, CMSX-8, and CMSX-4 Plus alloys in HPT blade use was developed using the method of finite element analysis (FEA). Analysis involved developing a suitable blade geometry, generating a good-quality mesh accounting for key zones, defining material properties accurately, and applying boundary conditions corresponding to realistic engine operating conditions.

3.1 Geometry

The blade geometry presented in Fig. 1 utilized in this analysis is a simplified high-pressure turbine blade section. It was optimized to maintain the essential aerodynamic

and structural features without redundant complexity. The model was a uniform thickness airfoil-shaped profile without internal cooling passages, enabling a straightforward focus on stress and strain behavior under load. Key features like the trailing edge and leading edge were properly preserved to mimic stress concentration regions common in actual turbine blades.

Fig. 1 Geometry of HPT Blade [21]

3.2 Mesh

A high-quality finite element mesh (Fig. 2) was created for the blade with tetrahedral elements, with further refinement in areas of importance like the leading edge, trailing edge, and blade root. While a mesh independence study was not specifically reported, the convergence of stress and deformation values in all simulations indicates that the mesh was adequately refined. Higher-order tetrahedral elements were used to capture the curvature and stress gradients in the complex geometry accurately.

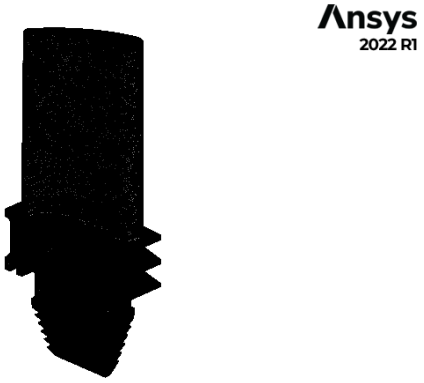

Fig. 2 Refined Mesh of Geometry after Convergence analysis

3.3 Materials

Material properties were defined from experimental data for CMSX-4, CMSX-8, and CMSX-4 Plus. All materials were treated as isotropic and independent of temperature for the scope of this simulation. The most important material properties utilized were density, coefficient of thermal expansion (CTE), Young's modulus, Poisson's ratio, tensile and compressive yield strengths, and ultimate strengths. CMSX-8 showed

slightly denser and stronger properties than CMSX-4, whereas CMSX-4 Plus provided intermediate performance between both, with strengthening and thermal stabilization. These properties of the material were essential for the precise forecast of stress and deformation behavior subjected to loads applied. These properties of the material were essential for the precise forecast of stress and deformation behavior subjected to loads applied. Material properties are listed in Tab. 1.

Tab. 1 Material Properties

Property	CMSX-4	CMSX-8	CMSX-4 Plus
Density [g/cm³]	8.7	9.0	8.85
Thermal Expansion Coefficient [CTE]	13.5×10^{-6}/K	13.2×10^{-6}/K	13.3×10^{-6}/K
Young's Modulus [GPa]	210	215	212
Poisson's Ratio	0.30	0.30	0.30
Tensile Yield Strength [MPa]	1 000	1 100	1 050
Compression Yield Strength [MPa]	1 000	1 100	1 050
Tensile Ultimate Strength [MPa]	1 100	1 200	1 150
Compression Ultimate Strength [MPa]	1 100	1 200	1 150

3.4 Boundary Conditions

The boundary conditions were carefully selected to simulate representative operating conditions of a high-pressure turbine blade. Structural constraint, the blade root, was completely restrained to simulate attachment to the turbine disc to preclude translation and rotation. Aerodynamic loading was simulated through imposition of uniform surface pressure over the blade airfoil to simulate flow-induced loads. In Fig. 3 the red colored surface is under action of force with arrow pointing to the direction of force and the blue surface is fixed.

For thermal loading, rather than taking a constant temperature across the blade, a prescribed one-dimensional parabolic temperature distribution along the blade span was used. The temperature profile was specified (Eq. 1) as a function of the spanwise coordinate s (from root at $s = 0$ to tip at $s = L$):

$$T(s) = T_{\min} + (T_{\max} - T_{\min}) \left\{ 1 - \left[\frac{s - aL}{bL} \right]^2 \right\} \tag{1}$$

where $T_{\min}$ and $T_{\max}$ are the root and tip blade temperatures, respectively. The parameter a was approximately 0.33, indicating that the maximum temperature occurs at about one-third of the blade length, consistent with observations for turbine blades. The spread parameter b was adjusted so that the root and tip temperatures matched the expected operating ranges of real turbine engines. The parabolic spanwise profile of this thermal distribution is a better representation of the uncooled turbine blade thermal environment than an assumption of uniform temperature. It guarantees that both thermal stresses and associated factors of safety distributions more closely follow physical expectations during service conditions. Such combined mechanical and thermal boundary conditions provided a sound basis for analyzing structural performance of considered alloys.

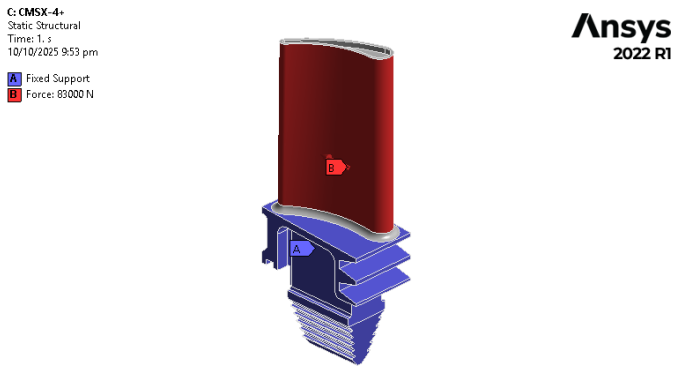

Fig. 3 Boundary conditions

4 Results

The structural behavior of the high-pressure turbine (HPT) blade, which was simulated using three different alloys, CMSX-4, CMSX-8, and CMSX-4 Plus, was examined in depth using finite element analysis (FEA). The analysis concentrated on some of the major output parameters: equivalent von Mises stress, strain, total deformation, and factor of safety (FOS) for each of the alloys. These parameters play a crucial role in determining the ability of the material to satisfy the stringent operating conditions present in turbine engines, where high temperatures and stress are a norm.

4.1 Stress

The similar von Mises stress distribution, which is an important factor in deciding the failure of the material, was found to be identical for each of the three materials under the applied loading conditions. The maximum von Mises stress developed across the entire blade for all materials was 8.496×10^8 Pa and stress distribution is identical as can be observed from Figs 4-6.

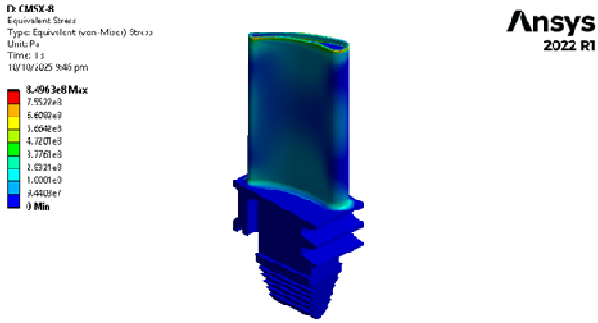

Fig. 4 Stress Contour of CMSX-8

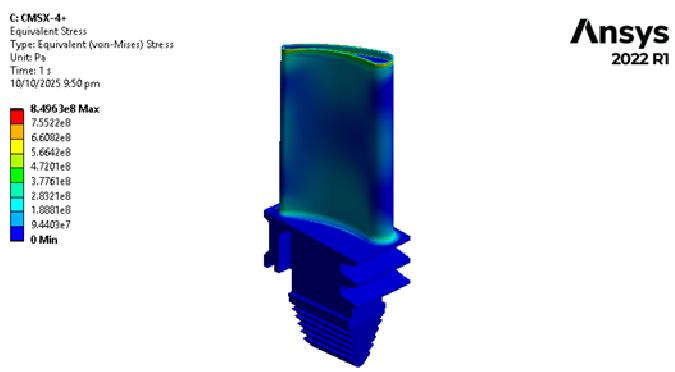

Fig. 5 Stress Contour of CMSX-4+

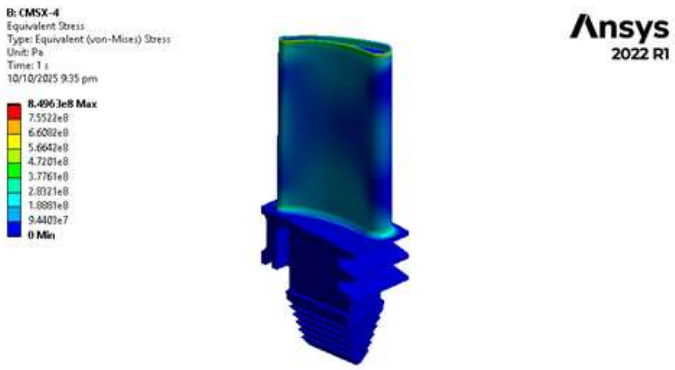

Fig. 6 Stress Contour of CMSX-4

This uniformity in stress distribution is because the used loads and boundary conditions of the FEA model are constant for the entire analysis. Therefore, the only parameter that influenced the results was the material properties. The von Mises stress was uniform for all the materials, even though. It must be remembered that stress itself cannot provide a complete representation of the overall performance of a material. Other factors such as strain, deformation, and factor of safety provide additional clues regarding the structural strength of the blade during working conditions.

4.2 Strain

The results exhibited extreme variation between the materials. Strain, or relative deformation from initial shape, is an important parameter to measure material performance. The material with the largest Young's modulus (a measure of stiffness) was CMSX-8, which registered the lowest value of strain at 3.952×10^{-3} (Fig. 7). This means that CMSX-8 would deform the least elastically under the load applied and therefore is most resistant to deformation among the three. CMSX-4 Plus ranked second with a strain value of 4.01×10^{-3} (Fig. 8). and CMSX-4 had the largest strain at 4.046×10^{-3} (Fig. 9). This difference in strain has a direct correlation with the relative

stiffness of these materials. The greater the stiffness (Young's modulus), the less deformation will result in a material when stressed. Thus, CMSX-8, being of higher stiffness, deforms the least, and this is a desirable property in high-performance uses like turbine blades.

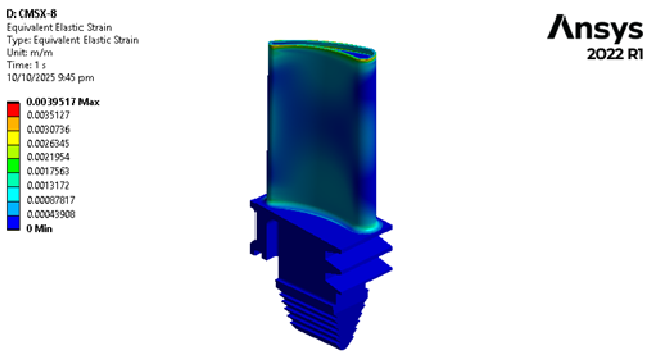

Fig. 7 Strain Contour of CMSX-8

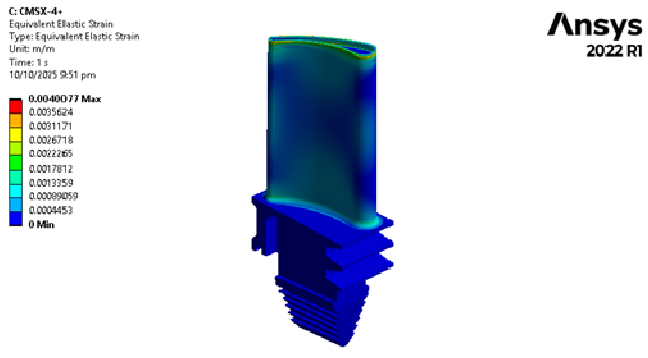

Fig. 8 Strain Contour of CMSX-4+

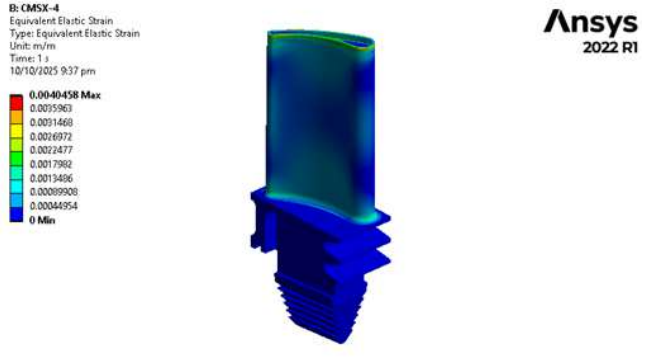

Fig. 9 Strain Contour of CMSX-4

4.3 Deformation

The sum of deformation, which measures the material displacement upon loading, also exhibited the same trend. CMSX-8 registered the smallest value of total deformation at 2.17×10^{-4} m (Fig. 10). CMSX-4 Plus, whose stiffness is comparatively high, yielded a slightly increased deformation of 2.21×10^{-4} m (Fig. 11), and CMSX-4 yielded the highest deformation of 2.23×10^{-4} m (Fig. 12). These findings again highlight the better stiffness behavior of CMSX-8, important for maintaining structural integrity of high-speed rotating turbine blades and thermally stressed blades. The reduced deformation in CMSX-8 implies that it is more efficient in sustaining its original shape during service stresses, hence reducing mechanical failure over time.

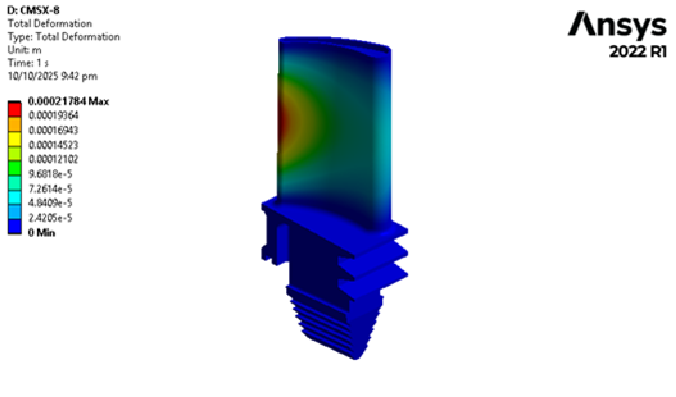

Fig. 10 Deformation Contour of CMSX-8

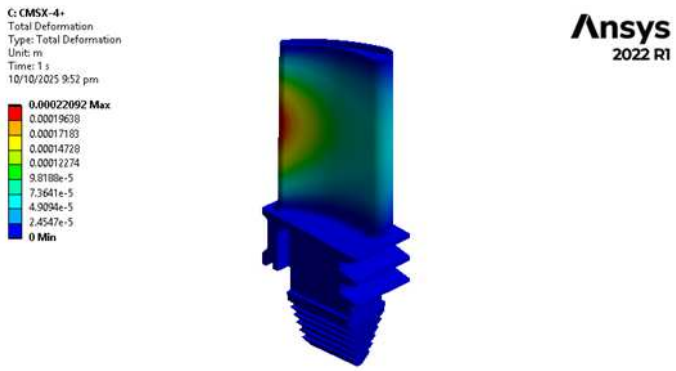

Fig. 11 Deformation Contour of CMSX-4+

4.4 Factor of Safety

The FOS can be computed by dividing the ultimate strength of the material by the maximum operating stress the material experiences. The higher the FOS, the higher the safety margin, and the material is less likely to fail under load. In this analysis, CMSX-8 achieved the highest FOS of 1.2947 (Fig. 13), indicating that it has the great-

est resistance to failure under the given loading conditions. CMSX-4 Plus came next with an FOS of 1.2358 (Fig. 14), which is also within the acceptable range, though lower than CMSX-8. CMSX-4, however, had the lowest FOS of 1.177 (Fig. 15), indicating that it has a reduced safety margin and is more susceptible to failure than the other two materials under identical conditions. The greater FOS for CMSX-8 indicates its better mechanical properties and capacity to resist higher stresses before failure, thus making it the strongest material for this application.

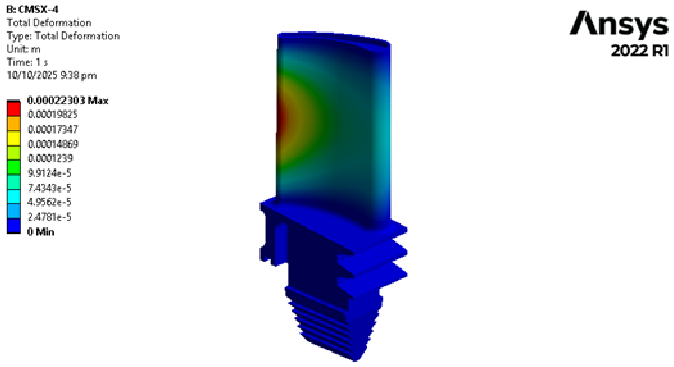

Fig. 12 Deformation Contour of CMSX-4

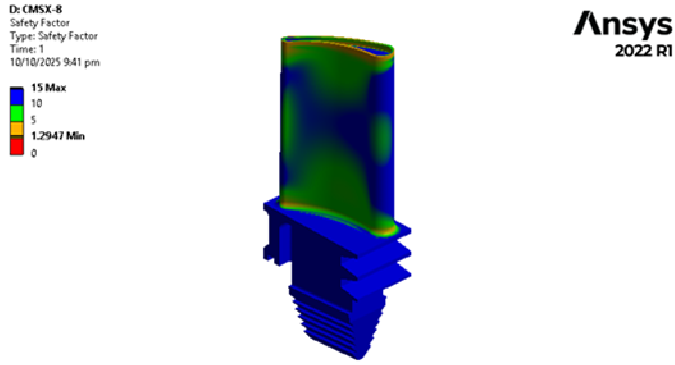

Fig. 13 FOS Contour of CMSX-8

Although all three materials, CMSX-4, CMSX-8, and CMSX-4 Plus, are subjected to the same stress levels under the given loads, the variations in their mechanical properties result in very large differences in strain, deformation, and factor of safety. CMSX-8 always proves to be superior to the other two materials as far as resistance to strain, deformation, and factor of safety is concerned, and is thus best suited for such high-performance and reliability-based applications as HPT blades in gas turbines. CMSX-4 Plus provides intermediate performance, with strain resistance and deformation being slightly better than in CMSX-4 but less than that of CMSX-8. These results highlight the significance of material choice in turbine blade design, where a combination of stiffness, strength, and safety is essential to guaranteeing long-term

operational reliability. Therefore, CMSX-8 emerges as the most beneficial material for high-performance turbine blades, with greater structural integrity and increased safety margin than CMSX-4 and CMSX-4 Plus. The results of the analysis are summarized in Tab. 2.

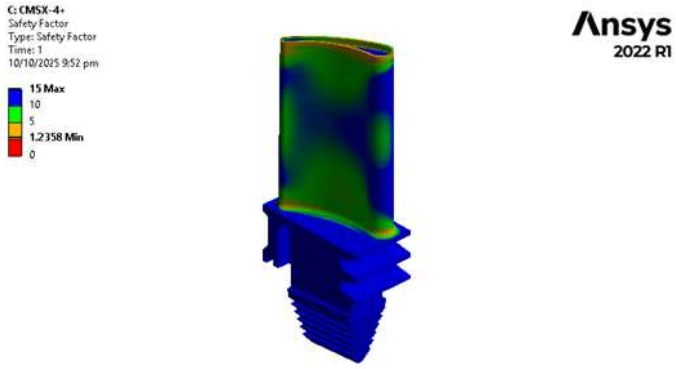

Fig. 14 FOS Contour of CMSX-4+

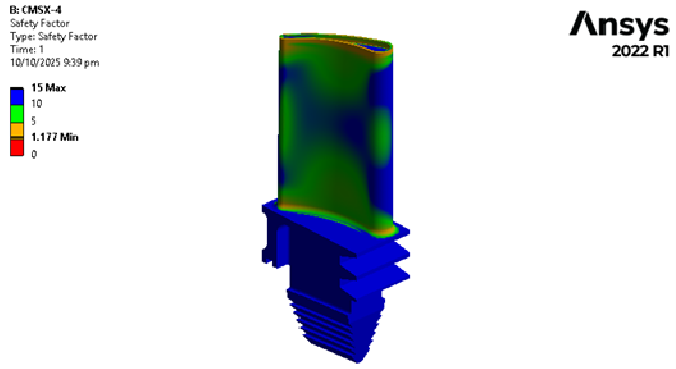

Fig. 15 FOS Contour of CMSX-4

Tab. 2 Summary of results

Property	CMSX-4	CMSX-8	CMSX-4 Plus
Strain	4.046×10^{-3}	3.952×10^{-3}	4.01×10^{-3}
Deformation [m]	2.23×10^{-4}	2.17×10^{-4}	2.21×10^{-4}
Factor of Safety	1.177	1.2947	1.2358
Stress [Pa]	8.496×10^{8}	8.496×10^{8}	8.496×10^{8}

5 Conclusion

This study successfully tested the structural reliability of a high-pressure turbine (HPT) blade using three advanced nickel-based single-crystal superalloys, i.e., CMSX-

4, CMSX-8, and CMSX-4 Plus. Through thorough finite element analysis, key performance parameters like equivalent stress, strain, deformation, and factor of safety were analyzed under real thermal and mechanical loading conditions.

The test results revealed that even though all three materials experienced equal levels of stress due to uniform loading, variation was considerable for strain, deformation, and margins of safety. CMSX-8 demonstrated the best overall structure performance in terms of minimum strain and deformation values and maximum factor of safety. This improved behavior is due to its alloy composition design with high rhenium content to enhance creep strength, stiffness, and mechanical toughness. CMSX-4 Plus contained improved properties over baseline CMSX-4 as a result of an even finer microstructure along with greater thermal stability though being less mechanically superior than CMSX-8.

The findings have the effect of reinforcing the significance of material choice in maximizing the strength and longevity of turbine blades employed in high-stress applications. Based on the evidence gathered in this study, CMSX-8 is the most suitable among the materials tested, having the best compromise of strength, stiffness, and safety suitable for application in high-pressure turbine blades.

Potential future work can involve creep and fatigue simulations for cyclically thermal loading, as well as assessments of material performance in actual blade geometries incorporating aspects like cooling passages and coatings.

References

[1] DUA, D., M. KHAJAVI, G. WHITE, D. THIRUMURTHY and J. SINGH. Stress Rupture Behavior of Disk Superalloys Exposed to Low-Temperature Hot Corrosion Environment. In: *ASME Turbo Expo 2020: Turbomachinery Technical Conference and Exposition*. New York: ASME, 2021. DOI 10.1115/GT2020-14113.

[2] ROZMUS-GÓRNIKOWSKA, M., J. KUSIŃSKI, Ł. CIENIEK and J. MORGIEL. The Microstructure and Properties of Laser Shock Peened CMSX-4 Superalloy. *Metallurgical and Materials Transactions A: Physical Metallurgy and Materials Science*, 2021, **52**(7), pp. 2845-2858. DOI 10.1007/s11661-021-06277-7.

[3] CHAPMAN, N., S. GRAY, J. SUMNER and J. NICHOLLS. Stress Corrosion Testing of CMSX-4, CM247LC DS and IN6203DS Ni-Base Superalloys. *Oxidation of Metals*, 2021, **95**(1-2), pp. 85-104. DOI 10.1007/s11085-020-10011-w.

[4] KUMAR, A., S. KUMAR and K.N. PANDEY. Life Prediction of C3X Gas Turbine Blade of CMSX-4 Material. *Advances in Materials and Processing Technologies*, 2022, **8**(4), pp. 4156-4180. DOI 10.1080/2374068X.2022.2039425.

[5] LÉTANG, M., S. BJÖRKLUND, S. JOSHI, D. SEBOLD, O. GUILLON and R. VAßEN. Repair of Single-Crystal CMSX-4 Using the High Velocity Air Fuel Process. *Journal of Thermal Spray Technology*, 2025, **34**, pp. 1489-1506. DOI 10.1007/s11666-025-01944-2.

[6] DURST, K. and M. GÖKEN. Micromechanical Characterisation of the Influence of Rhenium on the Mechanical Properties in Nickel-Base Superalloys. *Materials Science and Engineering: A*, 2004, **387-389**, pp. 312-316. DOI 10.1016/j.msea.2004.03.079.

[7] CHOI, B.G., C.Y. JO, H.U. HONG, I.S. KIM, S.M. SEO and H.M. KIM. Effect of Pre-Strain on Microstructural Evolution during Thermal Exposure of Single

Crystal Superalloy CMSX-4. *Transactions of Nonferrous Metals Society of China*, 2011, **21**(6), pp. 1291-1296. DOI 10.1016/S1003-6326(11)60855-8.

[8] XIA, W., et al. New Strategy to Improve the Overall Performance of Single-Crystal Superalloys by Designing a Bimodal γ′ Precipitation Microstructure. *Acta Materialia*, 2023, **257**, 119200. DOI 10.1016/j.actamat.2023.119200.

[9] SHANG, Z., et al. Microstructure and Mechanical Properties of a New Nickel-Based Single Crystal Superalloy. *Journal of Materials Research and Technology*, 2020, **9**(5), pp. 11641-11649. DOI 10.1016/j.jmrt.2020.08.032.

[10] SONG, Y., et al. New Insights into the Optimisation of the Solution Heat Treatment Process and Properties of CMSX-4 Superalloys. *Materials Science and Engineering: A*, 2024, **890**, 145947. DOI 10.1016/j.msea.2023.145947.

[11] CHENG, Y., X. ZHAO, W. XIA, Q. YUE, Y. GU and Z. ZHANG. The Overview of the Formation Mechanisms of Topologically Close-Packed Phases in Ni-Based Single Crystal Superalloys. *Materials and Design*, 2024, **237**, 112582. DOI 10.1016/j.matdes.2023.112582.

[12] WANG, T., et al. Effect of Temperature on Tensile Behavior, Fracture Morphology and Deformation Mechanisms of Nickel-Based Single Crystal CMSX-4. *Journal of Alloys and Compounds*, 2022, **912**, 165175. DOI 10.1016/j.jallcom.2022.165175.

[13] LI, Y.M., et al. Carbon Addition and Temperature-Dependent Tensile Deformation Resistance and Capacity of a Low-Cost 3rd-Generation Ni-Based Single Crystal Superalloy. *Materials Characterization*, 2024, **210**, 113794. DOI 10.1016/j.matchar.2024.113794.

[14] WIJEYERATNE, N., F. IRMAK, N. O'NORA and A.P. GORDON. A Comparative Study of Constitutive Modeling of an Aero-Engine Single Crystal Superalloy under Creep-Thermomechanical Fatigue. In: *AIAA Science and Technology Forum and Exposition, AIAA SciTech Forum 2022*. Reston: AIAA, 2022. DOI 10.2514/6.2022-0629.

[15] HARRIS, K. and S. CANNON. CMSX-4® Plus Single Crystal Alloy Development, Characterization and Application Development. In: *Proceedings of the 13th International Symposium on Superalloys*. Pittsburgh: The Minerals, Metals & Materials Society, 2016. DOI 10.1002/9781119075646.ch3.

[16] LI, D., et al. High Temperature Oxidation Behavior of Ni-Based Superalloy Nimonic 95 and the Effect of Pre-Oxidation Treatment. *Vacuum*, 2021, **194**, 110582. DOI 10.1016/j.vacuum.2021.110582.

[17] TARASOV, D., A. TYAGUNOV and O. MILDER. Simulation of the Nickel Superalloys Solvus Temperature by the Deep Learning Artificial Neural Network with Differential Layer. In: *AIP Conference Proceedings*, 2022, **2611**(1), 130008. DOI 10.1063/5.0119488.

[18] WU, R.T. and R.C. REED. On the Compatibility of Single Crystal Superalloys with a Thermal Barrier Coating System. *Acta Materialia*, 2008, **56**(3), pp. 313-323. DOI 10.1016/j.actamat.2007.07.057.

[19] LI, D., et al. Long-Term Aging Behavior and Mechanism of CMSX-4 Nickel-Based Single Crystal Superalloy at 950 °C and 1050 °C. *Journal of Alloys and Compounds*, 2024, **1004**, 175763. DOI 10.1016/j.jallcom.2024.175763.

[20] ESTRADA RODAS, E.A., S. GORGANNEJAD and R.W. NEU. Creep-Fatigue Behaviour of Single-Crystal Ni-Base Superalloy CMSX-8. *Fatigue and Fracture of Engineering Materials and Structures*, 2019, **42**(9), pp. 2155-2171. DOI 10.1111/ffe.13098.

[21] KUKLA, D., M. KOPEC, R. SITEK, A. OLEJNIK, S. KACHEL and Ł. KISZKOWIAK. A Novel Method for High-Temperature Fatigue Testing of Nickel Superalloy Turbine Blades with Additional NDT Diagnostics. *Materials*, 2021, **14**(6), 1392. DOI 10.3390/ma14061392.